The impregnation of mesoporous silica with diaminohexane by means of supercritical CO2: A possible CO2 solid sorbent

Original
The impregnation of mesoporous silica with diaminohexane by means of supercritical CO2: A possible CO2 solid sorbent / Gallo, M., Ronchetti, S., Onida, B., Manna, L.. - In: JOURNAL OF CO2 UTILIZATION. - ISSN 2212-9820. - 101:(2025). [10.1016/j.jcou.2025.103207]

Publisher:
Elsevier

Published
DOI:10.1016/j.jcou.2025.103207

Journal of CO2 Utilization 101 (2025) 103207

Contents lists available at ScienceDirect

Journal of CO2 Utilization

journal homepage: www.elsevier.com/locate/jcou

The impregnation of mesoporous silica with diaminohexane by means of supercritical CO_2: A possible CO_2 solid sorbent

Marta Gallo *, Silvia Ronchetti, Barbara Onida, Luigi Manna

Dipartimento di Scienza Applicata e Tecnologia, Politecnico di Torino, Corso Duca Degli Abruzzi, 24, Torino 10129, Italy

ARTICLE INFO

Keywords:
Sorbents
CO_2 capture
Supercritical CO_2
Amine
Silica

ABSTRACT

Among solid sorbents, silica is particularly interesting thanks to its stability and versatility. With this in mind, we developed a silica sorbent impregnated with amino groups to increase its ability to capture CO_2. A commercial mesoporous silica (type SBA-15) was impregnated with a diamine (diaminohexane) by using supercritical CO_2 as a green solvent. The so obtained sorbent was physico-chemically characterized and its adsorption behavior was investigated by means of volumetric isotherms at room temperature (and data were fitted by Langmuir models) and *in situ* Fourier Infrared Spectroscopy. The results prove that the impregnation with supercritical CO_2 is effective and the resulting material is able to capture CO_2. Although the CO_2 capture capacity value of the impregnated material is comparable to that of the pristine one (0.89 mmol/g and 0.94 mmol/g, respectively, at 25 °C), the impregnated sorbent is significantly more efficient in capturing CO_2 at low pressure. Chemisorption and, secondary, physisorption are observed. Both phenomena are reversible at room temperature, allowing an easy regeneration of the sorbent. The material, moreover, is stable also at higher temperature, proving to be compatible with thermal regeneration processes. Finally, Langmuir modeling indicates a dual-site behavior, with stronger adsorptions sites attributed to amines, and weaker sites attributed to silica.

1. Introduction

As it is already well known, CO_2 is a greenhouse gas and its concentration has dramatically increased since the Industrial Revolution, passing from 280 ppm to more than 420 ppm in recent years [1]. The resulting climate changes are already affecting millions of people around the world, and the effects will be even more severe if the causes of climate change are not drastically reduced [2].

The envisaged long-term solutions include a drastic cut in CO_2 emissions, involving a radical change in many of the current paradigms (of production, of life…). In the meantime, transition solutions are sought for.

Among these, the recovery of CO_2 is widely investigated. The currently adopted strategy is the so-called wet-scrubbing with liquid amines, where amine solutions interact with gaseous CO_2 through acid-base reactions forming species highly soluble in solution, so depleting the gas stream of CO_2 [3]. This process is highly selective and effective; however, the regeneration of the amine solution is high energy demanding since it takes place at 100–140 °C [4]. If accidentally released, amines can cause adverse effects on human health and the environment [5]. Moreover, amine solutions are highly corrosive, and their use induces elevated maintenance costs [6]. Finally, amines easily undergo oxidative degradation, a phenomenon that gradually decreases the efficiency of the wet-scrubbing process [6].

To overcome these limitations, alternative strategies are currently studied. A promising alternative is offered by solid sorbents, since these are easy to produce, to regenerate, and to handle. Among solid sorbents, the most studied ones are activated carbons, zeolites, metal-organic frameworks (MOF), and porous silica [7].

Although being efficient in CO_2 removal and requiring lower regeneration energies than liquid amines, also the solid sorbents present some drawbacks. In particular, activated carbons suffer from a strong variability of properties depending on their precursor material; moreover, their regeneration often requires high heat [8]. MOF are costly and difficult to produce on large scale [8]. Zeolites have an adsorption efficiency that decreases in the presence of moisture and impurities in gas feed [9], and have low selectivity [10]. Porous silica, being less prone to these limitations, represents a valid alternative. To increase the ability (kinetics, selectivity…) of silica to capture CO_2, a possible strategy is to functionalize it with functional groups that can chemically interact with

---

* Corresponding author.
E-mail address: marta.gallo@polito.it (M. Gallo).

https://doi.org/10.1016/j.jcou.2025.103207
Received 23 February 2025; Received in revised form 16 August 2025; Accepted 20 August 2025

CO_2, such as amines.

In the present study, we used a commercial mesoporous silica (SBA-15) as a support and we selected a di-amine, diaminohexane (DH), as functionalizing agent. It is worth mentioning that, based on the literature on amino-modified mesoporous silica [11], it is known that two amino groups are necessary to form carbamate species by interaction with one CO_2 molecule. In this sense, we selected on purpose a diamine with an alkyl chain long and flexible enough to fold and ideally interact with CO_2 with both its amine groups. In addition, previous studies report that the energy barrier for the reaction between CO_2 and amines, which is a key factor affecting CO_2 adsorption, is favorably lower for amines with longer alkyl chain (up to six carbon atoms, such as DH [12,13]). Finally, compared to other amines, DH has advantages such as lower price and higher boiling point [14]; moreover, DH solutions have been already proved promising for CO_2 capture [15]. Although these advantages, few studies are present in the literature about its use for CO_2 capture either in form of liquid amine solution [15] or as a functionalizing agent. The few examples of CO_2 sorbents functionalized with DH are limited to volcanic tuff [13], multi-walled carbon nanotubes (MWCNTs) [14] and silica [16]. However, in all these studies, the sorbent preparation requires the use of polluting solvents, such as methanol [16], and preliminary treatments, such as activation [13] or oxidation [14], which involve energy consumption (treatment at 50–90 °C [13,14]) as well as time consumption (up to 24 h [14]).

The innovative approach presented in this work consists in using supercritical CO_2 ($scCO_2$) as a solvent for the functionalization process, thus avoiding the use of polluting organic solvents and offering a relatively simple alternative. To the authors' knowledge, this is the first time that a DH-functionalized silica sorbent is obtained by impregnation with $scCO_2$.

The DH-functionalized sorbent obtained by $scCO_2$ impregnation, as well as the reference pristine silica, were characterized in terms of physico-chemical properties and their efficacy in adsorbing CO_2 was studied by means of volumetric isotherms at room temperature. The so obtained data were regressed by Langmuir models (Single-Site and Dual-Site). Moreover, the interaction between the sorbent surface and CO_2 molecules was analyzed by means of *in situ* IR spectroscopy.

2. Materials and methods

For the synthesis and characterization of the samples the following chemicals were used (as received): mesoporous silica SBA-15 with pore size 8 nm (Sigma Aldrich, Burlington, MA, USA), 1,6-diaminohexane ($C_6H_{16}N_2$, DH) in powder (Sigma Aldrich, Burlington, MA, USA), ethanol (absolute ethanol, for analysis, Merck, Darmstadt, Germany). According to the producer, the properties of DH are: MM = 116.20 g/mol, T_f = 39–42 °C, T_b = 199–204 °C, density = 0.83 cm^3/g at 60 °C.

For the functionalization process, a physical mixture of DH (21 mg) and silica (200 mg) in a proportion of 50 mmol DH/mol SiO_2 (chosen on the base of a previous work [17]) was manually prepared. The mixture was poured in a package made of filter paper and placed in a glass vial disposed in a 40 mL stainless steel vessel (with an internal diameter of 14 mm). The vessel was filled with liquid CO_2; temperature and pressure were adjusted to 40 °C and 200 bar, to overcome the critical point of CO_2. In these conditions, CO_2 acted as a solvent dissolving DH. The mixture was kept at these temperature and pressure for 2 h to allow the dissolution of DH and its diffusion in the porosity of silica. Then, pressure was slowly release (around 5 mL/min) and CO_2 passed from supercritical to gaseous state; once below the critical point, the solubility of DH in CO_2 rapidly decreased and DH precipitated on the spot (i.e., inside the silica). Finally, the vessel was left to naturally cool down.

For comparison, a further absorbent was obtained by traditional impregnation (incipient wetness impregnation). For this purpose, a solution of ethanol (1.5 mL) and DH (47 mg) was prepared; 0.66 mL of it were administered to 200 mg of silica (SBA-15 with pore size 8 nm). Then, the solvent was let to evaporate. At the end of the loading process, 21 mg of DH were theoretically added to 200 mg of silica.

The amine-impregnated samples, as well as the pristine silica (as a reference) were analyzed as follow.

Thermogravimetric (TGA) analyses were carried out using a Setaram TGA (Caluire, France) by heating the samples between 20 °C and 600 °C with a heating rate of 10 °C/min in air flow. An isotherm test was carried out for assessing the thermal stability of the specimens (inspired by [18]): samples were heated at 10 °C/min in air flow until they reached 120 °C and then they were left at a constant temperature of 120 °C for 1 h.

X-Ray diffraction (XRD) data were collected using an Empyrean (Cu Kα radiation, Malvern Panalytical, Almelo, The Netherlands), at 40 kV and 40 mA, with a solid-state detector (PIXcel1D). Measurements were performed at low (2θ = 0.7°-5°) and high angles (2θ = 5°-60°).

FTIR spectra were recorded at a resolution of 2 cm^{-1} on pelletized powders using an Equinox 55 spectrometer (Bruker, Billerica, MA, USA) after outgassing the sample at room temperature (residual pressure of 0.1 Pa).

Nitrogen adsorption-desorption isotherms were acquired using an ASAP 2020 Plus analyzer (Micromeritics, Norcross, GA, USA). Samples were outgassed at 70 °C in a nitrogen atmosphere at a pressure of 10 mmHg for 3 h. The surface area was calculated using the Brunauer–Emmett–Teller (BET) method [19], and pore volume using the Barrett–Joyner–Halenda (BJH) method [20], using desorption isothermal data.

Volumetric adsorption of CO_2 was evaluated with the same instrument used for nitrogen isotherms. In this case, samples were outgassed at 120 °C for 2 h and the measures were carried out at 25 °C. Two runs of measurement were carried out, with a 1 h outgassing at room temperature between the first and the second run.

In situ FTIR analyses were performed exposing the samples at different CO_2 equilibrium pressures at room temperature. The samples were outgassed beforehand at 120 °C for 2 h. At the end of the test the samples were outgassed at room temperature (under vacuum) for 5 min and a final FTIR spectrum was acquired.

3. Results

Fig. 1 reports FTIR spectra of the pristine silica, SBA_ref, and the sample functionalized with diaminohexane, SBA_DH. The spectrum of the reference material presents bands typical of amorphous silica, i.e. a narrow band above 3700 cm^{-1}, mainly due to free terminal silanols, and a broad band between 3300 and 3600 cm^{-1}, due to silanols mutually interacting by H-bond. The spectrum of the functionalized sample is significantly different, with no band due to free terminal silanols. Moreover, the appearance of new bands is noted. Specifically, two peaks at about 3300 cm^{-1}, due to $-NH_2$ stretching modes, a band at about 1600 cm^{-1}, due to the $-NH_2$ bending mode, and two bands in the range

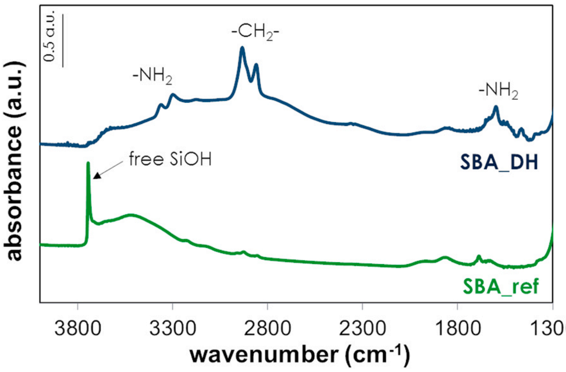

Fig. 1. FTIR spectra of the reference sample, SBA_ref, and the functionalized sample, SBA_DH.

2800–2900 cm^{-1}, ascribed to -CH_2- stretching modes [21]. Furthermore, a broad absorption between 2500 and 3600 cm^{-1} is observed, to which the stretching modes of -NH_2 and -CH_2- are superimposed. This absorption is ascribed to the stretching mode of silanols engaged in H-bonding with -NH_2 groups of adsorbed diaminohexane molecules [22].

The mass losses recorded by means of TGA are reported in Fig. 2. Below 150 °C SBA_ref loses 2.0 wt% due to evaporation of physisorbed water, while the mass loss between 150 °C and 600 °C is 1.3 wt% and can be ascribed to the condensation of silanols [23]. SBA_DH loses 4.5 wt% of water below 150 °C and 12.5 wt% between 150 °C and 600 °C. This latter mass variation can be attributed to the degradation of the incorporated amine and, at the same time, to the condensation of silanols. Considering the contribution due to silanols condensation equal to that measured on the pristine silica (1.3 wt%), the weight loss due to the amines degradation turns out to be 11.2 wt%.

Textural properties of the samples were assessed by nitrogen adsorption at 77 K. The main results are reported in Fig. 3 and Table 1. Both the reference and the functionalized sample present type IV isotherm, with H1 hysteresis loop typical of mesoporous materials with ordered and uniform cylindrical pores (Fig. 3A) [24]. This is confirmed by the narrow pore diameter distribution, obtained according to the BJH model [20] and reported in Fig. 3B. After functionalization, the specific surface area, the pore volume, and the average pore diameter decrease, as reported in Table 1, but the pore distribution remains narrow. These results are coherent with a uniform functionalization of the inner pore walls, without relevant pore blocking phenomena [25].

SBA_DH was compared to a sorbent obtained by a traditional impregnation technique (i.e., incipient wetness impregnation – IWI). The two samples were prepared using the same initial quantities of silica and DH, so to have the same nominal content of diamine. The textural properties and the measured DH-content of the sorbent obtained by IWI (Table A.1) were less apt to adsorption than those of SBA_DH, therefore the CO_2 adsorption tests were carried out only on the SBA_DH sample.

CO_2 adsorption performances were evaluated by volumetric adsorption isotherms at 25 °C (RT). For each sample two consecutive runs were performed; a 1-hour outgas at room temperature was carried out between the first and the second run to remove the species reversibly adsorbed. The resulting isotherms are reported in Fig. 4A and B for SBA_DH and SBA_ref, respectively. In both cases, the two runs are almost completely superimposed, suggesting that the adsorption phenomena are reversible on both samples.

A direct comparison of the first run on SBA_ref and SBA_DH is reported in Fig. 4C: although both curves reach roughly the same maximum adsorbed value (0.94 mmol/g for SBA_ref and 0.89 mmol/g for SBA_DH), they display a significantly different trend. The isotherm of SBA_DH is characterized by a downward concavity and a drastic increase of CO_2 adsorption in the lowest pressure range (Fig. 4D). Moreover, for pressures lower than approximately 700 mbar, SBA_DH shows a higher CO_2 adsorption than SBA_ref at the same equilibrium pressure.

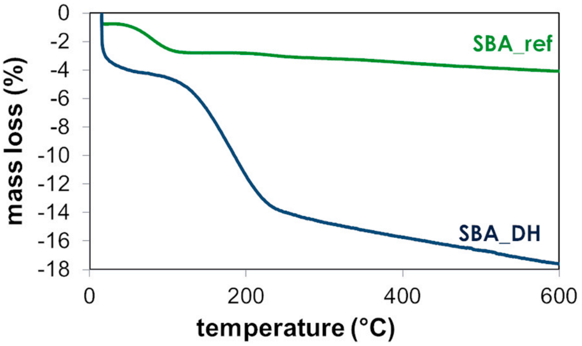

Fig. 2. Thermogravimetric curves of the reference sample, SBA_ref, and the functionalized sample, SBA_DH.

All experimental data were fitted to adsorption isotherm models using the least squares method. In the case of the pure silica sample, SBA_ref (Fig. 5B), the classical Single-Site Langmuir equation [26] provided an excellent fit to the experimental data, with an adjusted R-squared of 0.9997 and a percent Average Absolute Relative Deviation (AARD%) of 2.8 %. The equation applied was:

$$n_{ads} = (n_{max} \cdot K \cdot P) / (1 + K \cdot P) \qquad (1)$$

where n_{ads} is the amount of CO_2 adsorbed (mol), n_{max} is the monolayer adsorption capacity (mol), K is the Langmuir equilibrium constant ($mbar^{-1}$), and P is the equilibrium pressure (bar).

For the functionalized sample, SBA_DH (Fig. 5A), the experimental data were fitted to several of the most widely used three- and four-parameter isotherm models reported in the literature. The three-parameter models of Sips [27], Redlich–Peterson [28], and Radke–-Prausnitz [29], which describe intermediate adsorption behavior between the Langmuir and Freundlich isotherms, produced similar performance, each with an AARD% of approximately 5 %. The Toth model [30] yielded a slightly higher AARD% value of 7.7 %. Slight improvements were observed using the four-parameter Marczewski–Jaroniec model [31], which extends the Toth equation to account for broader energetic heterogeneity among adsorption sites, achieving an AARD% of approximately 5 %. The purely empirical four-parameter model proposed by Fritz–Schlunder [32] provided comparable results.

The best fit to the experimental data was obtained using a Dual-Site Langmuir model [26,33], which achieved an AARD% of 2.7 %. The applied equation is given as:

$$n_{ads} = (n_{max} \cdot K \cdot P) / (1 + K \cdot P) + (n'_{max} \cdot K' \cdot P) / (1 + K' \cdot P) \qquad (2)$$

where n_{max} and K refer to the maximum adsorption capacity and equilibrium constant for the first type of adsorption site, and n'_{max} and K′ refer to those for the second site.

It is worth noting that the Langmuir model is of particular interest, since it provides additional evidence regarding the properties of the material (i.e., number of adsorbing sites, strength of interaction).

As shown in Fig. 5, the fitted curves (light blue and light green lines in Figs. 5A and 5B, respectively) match the experimental data (dotted lines) very well. The corresponding values of the optimized parameters, adjusted R-squared, AARD%, and Root Mean Square Deviation (RMSD) between experimental and fitted data are summarized in Table 2.

The interaction between CO_2 and the samples was studied through *in situ* FTIR spectroscopy. Fig. 6 shows the difference spectra, related to increasing CO_2 equilibrium pressures, obtained by subtracting to each spectrum the one recorded prior to CO_2 adsorption (i.e., spectra reported in Fig. 1). Moreover, the spectrum recorded after outgassing (under vacuum) at room temperature to remove the adsorbed CO_2 is also reported (dashed curve, “degas”).

In the SBA_ref spectra, a peak appears at around 2340 cm^{-1} and its intensity increases with increasing CO_2 pressure (Fig. 6). This peak is due to molecular CO_2 [34], which is pysisorbed on the silica surface through weak interactions. When SBA_ref is outgassed at room temperature, this peak disappears (dashed line in Fig. 6), confirming that the physisorption phenomenon is completely reversible at room temperature.

At variance with SBA_ref, in the case of SBA_DH, besides the band due to molecular CO_2, new bands appear in the range 1500–1600 cm^{-1} (inset in Fig. 6). These can be attributed to the formation of carbamates [11,35] caused by the chemical interaction between the basic amine groups of DH and the acid CO_2. Chemisorption of CO_2 forming carbamates is also reversible at room temperature and the outgassing is sufficient to desorb CO_2 (dashed line in the inset of Fig. 6).

Even though the adsorption of CO_2 was reversible at room temperature, for sake of completeness, in view of a possible thermal regeneration of the adsorbent, the thermal stability of the functionalised sample

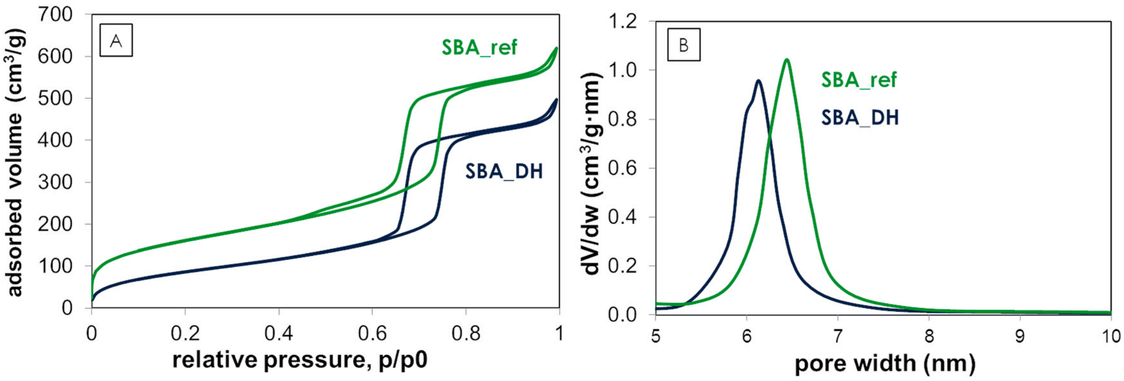

Fig. 3. Nitrogen adsorption isotherms (A) and pore size distribution (BJH model) (B) of the reference sample, SBA_ref, and the functionalized sample, SBA_DH.

Table 1
Textural properties of the reference sample, SBA_ref, and the functionalized sample, SBA_DH.

	SBA_ref	SBA_DH
Specific surface area (m^2/g)	570	330
Pore volume (cm^3/g)	0.9	0.7
Average pore diameter – BJH (nm)	6.4	6.1

was assessed with an isothermal thermogravimetry test at 120 °C for 1 h. The results, reported in Fig. 7, reveal that, after an initial mass loss due to the desorption of physisorbed water, the sample is stable and only a negligible mass loss (0.5 wt%) takes place for the whole duration of the test.

4. Discussion

The characterization analyses prove that the amine is successfully incorporated by means of $scCO_2$ on the silica support. The presence of DH is testified by FTIR spectra (Fig. 1), where the functional groups typical of DH (-NH_2 and -CH_2-) are clearly visible. FTIR also suggests H-bond interactions between silica and DH (coherent with the broad band between 2500 and 3600 cm^{-1}). Together with data from nitrogen sorption isotherms, this evidence strongly suggests that DH molecules are homogeneously distributed on the silica surface of the inner pore wall. As expected, the SSA and the pore volume of the functionalized sample are lower than those of the reference specimen. Nevertheless, SBA_DH still presents an isotherm typical of mesoporous materials, with SSA, pore volume, and pore diameter suitable to the final application. The amount of DH experimentally measured by TGA (11.2 wt%, Fig. 2)

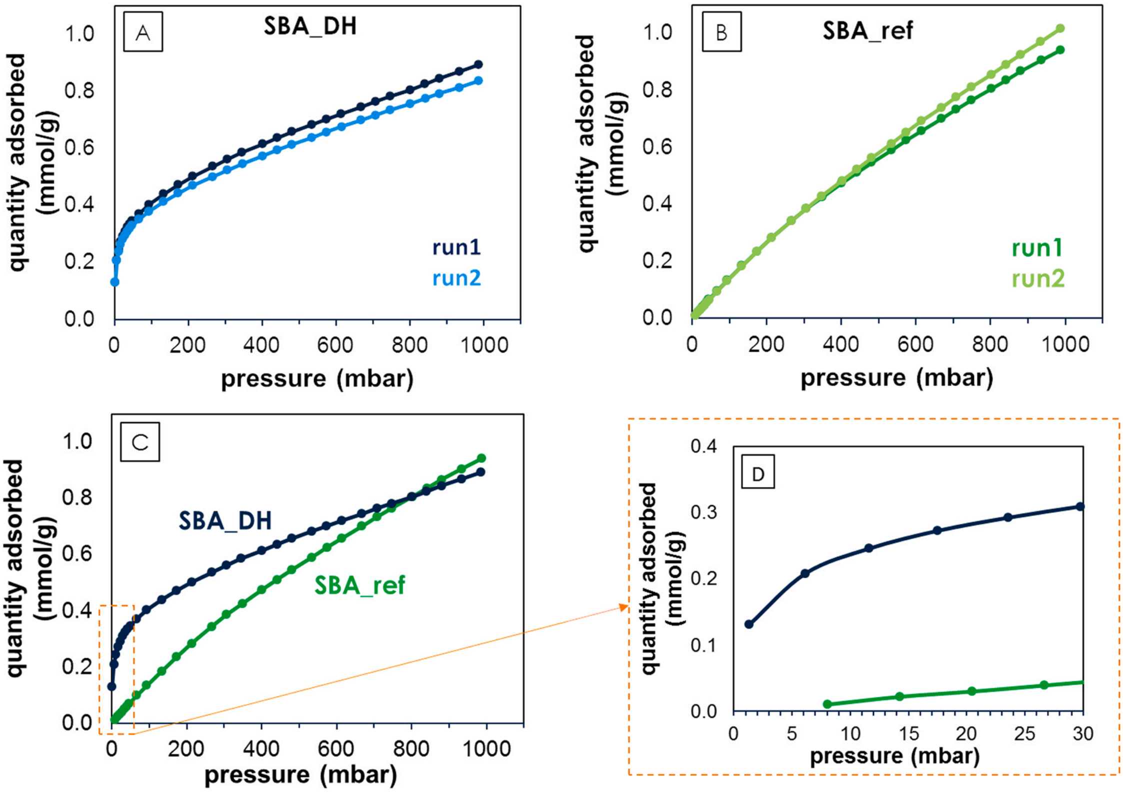

Fig. 4. Volumetric CO_2 adsorption isotherms at RT of the functionalized sample, SBA_DH (A), and the reference sample, SBA_ref (B), and the comparison of the two (C) with a zoom on the lowest pressures range (D).

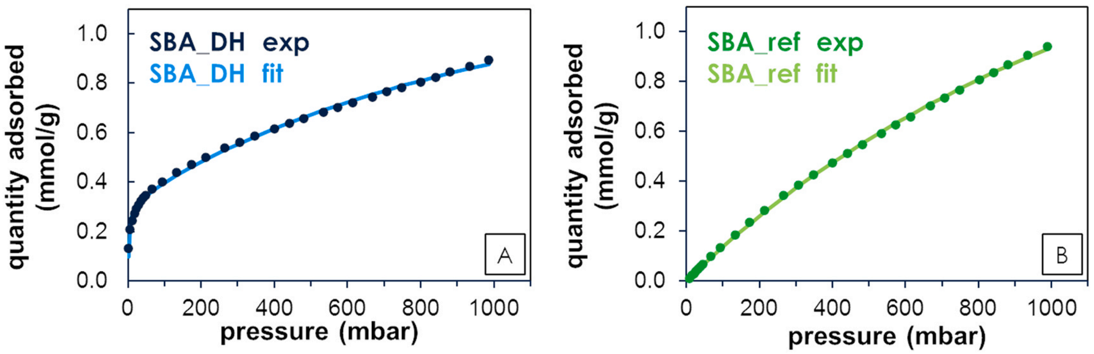

Fig. 5. Fitting of the volumetric CO_2 adsorption curves of the functionalized sample, SBA_DH (A), and the reference sample, SBA_ref (B).

Table 2
Fitting parameters of the volumetric CO_2 adsorption isotherms.

	n_{max} (mmol/g)	K (mbar^{-1})	n'_{max} (mmol/g)	K' (mbar^{-1})	adjusted R-squared	AARD% (%)	RMSD (mmol/g)
SBA_ref	2.69	$5.34 \cdot 10^{-4}$	-	-	0.9997	2.8	0.006
SBA_DH	1.35	$7.22 \cdot 10^{-4}$	0.315	0.332	0.9976	2.7	0.011

is very close to the nominal one (10 wt%), suggesting that the loading technique prevents loss of the functionalizing agent. On the overall, the physico-chemical properties of SBA_DH are more favorable than those of a similar sorbent obtained with a traditional impregnation technique (Table A.1), supporting the interest of the alternative approach proposed in this work.

Adsorption isotherms show that SBA_DH is able to adsorb CO_2 at room temperature. For high CO_2 pressure its adsorption capacity is comparable to that of the reference material (Fig. 4). However, it is worth underlining that, at low CO_2 pressure, the amount adsorbed by SBA_DH is significantly higher than that of SBA_ref: for example, at around 100 mbar SBA_ref adsorbs 0.1 mmol/g, while SBA_DH adsorbs 0.4 mmol/g (Fig. 4C). In particular, the concavity of the volumetric isotherms suggests a specific interaction between SBA_DH and CO_2 (Fig. 4A), which, however, is completely reversible at room temperature (since run 2 overlaps run 1 in volumetric measurements). These observations are confirmed by *in situ* FTIR measurements. When SBA_ref is in contact with increasing amounts of CO_2 it only interacts through weak interactions that result in the physisorption of molecular CO_2 on the silica surface. On the other hand, when SBA_DH is in contact with CO_2, the amine groups interact with CO_2 also through the formation of new chemical species (i.e., carbamates) inducing a chemisorption phenomenon already at low pressure. Although the interaction between SBA_DH and CO_2 is due to chemical bonds (at least partially), the adsorption phenomenon is reversible at room temperature. It may be surprising, but, as reported in the literature, carbamate formation may be reversible even at room temperature in some conditions (such as when applying vacuum [36,37]). In the present case, indeed, an outgassing at room temperature for a few minutes is sufficient for the adsorbent regeneration, coherently with what observed in the volumetric tests.

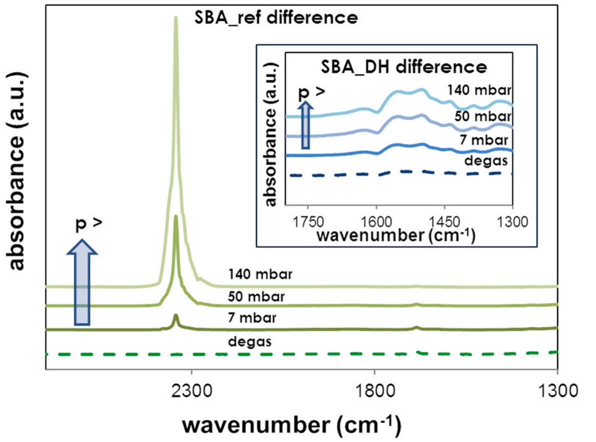

Fig. 6. In situ FTIR difference spectra at different CO_2 pressures for the reference sample, SBA_ref, and the functionalized sample SBA_DH (inset).

It is worth noting that the reversibility of the adsorption phenomena on SBA_DH is coherent with the lack of any CO_2 residue on the samples after the $scCO_2$ impregnation. This result further confirms the validity of the $scCO_2$ impregnation: after the impregnation process, the active sites are free, and no further treatments are necessary to make them available to interact with CO_2.

The fitting of the volumetric isotherms with a Langmuir model supports the outcomes of the *in situ* FTIR tests. In the case of SBA_ref a simple single-site Langmuir model well fits the experimental data, indicating that one type of interaction occurs between the surface of the silica and CO_2 molecules, i.e., the physisorption in the linear molecular form observed by *in situ* FTIR characterization (Fig. 6A). In the case of SBA_DH, instead, a Dual-Site Langmuir model is necessary: the weak interaction between silica and CO_2, as observed for SBA_ref, is represented by the first site (n_{max} and K), while the amine groups, which interact with CO_2 forming carbamate species, are represented by the second site (n'_{max} and K'). Indeed, the K parameters of the SBA_ref

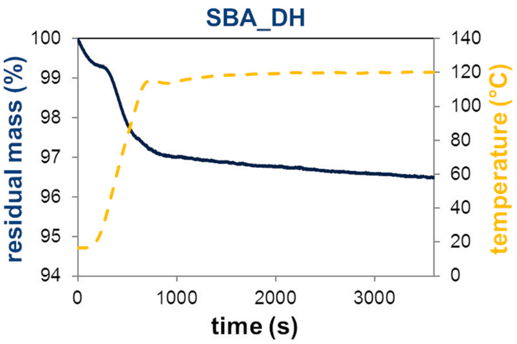

Fig. 7. Thermogravimetric curve of the functionalized sample, SBA_DH, for in isotherm treatment at 120 °C.

Table 3
Comparison of the CO_2 adsorption capabilities exhibited by SBA_DH and comparable materials.

sample	DH content (wt%)	Adsorption T (°C)	CO_2 capture (mmol/g)	Reference
Volcanic tuff + DH	70	25	0.98	[13]
SBA + DH	30	45	1.24	[16]
SBA + DH	10	25	0.89	this work

Langmuir equation (K= $5.34 \cdot 10^{-4}$ $mbar^{-1}$, Table 2) and of the first site of SBA_DH Dual-Site Langmuir equation (K= $7.2 \cdot 10^{-4}$ $mbar^{-1}$, Table 2) are comparable, indicating that the strength of the interaction is similar for the two adsorbing sites. However, n_{max} for SBA_ref is higher than that of SBA_DH (n_{max}=2.69 mmol/g and n_{max}=1.35 mmol/g, respectively, Table 2), coherently with its higher SSA (Table 1). Interestingly, the ratio between the two values, which represent the total amount of adsorbing sites, is very close to the ratio between the SSA values of the two adsorbents.

Regarding the second site obtained for SBA_DH by the Dual-Site Langmuir model, it is worth noting that its equilibrium constant, K' (0.33 $mbar^{-1}$), is significantly higher than that of the first site K ($7.2 \cdot 10^{-4}$ $mbar^{-1}$) coherently with the fact that this second site is responsible for the chemical interaction forming carbamate. The total amount of sites, n'_{max}, turns out to be 0.315 mmol/g from the Langmuir equation; this value can be compared to the total amount of DH in the adsorbent.

Considering the nominal value of DH content, which is 10 wt%, this corresponds to 0.830 mmol/g.

The nominal total amount of DH, expressed in mmol of DH per gram of adsorbent, is higher than n'_{max}, which, according to the Dual-Site Langmuir model, indicates the maximum amount absorbed on the stronger adsorbing sites, which are considered responsible for the carbamate formation. This is not surprising if one takes into account at least two considerations. First, based on the literature [11], we should expect that both the amino groups of the DH molecule interact with one CO_2 molecule to form the carbamate species. This involves that the adsorbing DH molecule is in a suitable configuration, which cannot be the case for all the molecules on the silica surface. The second consideration regards the evidence of H-bonding between the surface silanols and the amino groups. It cannot be ruled out that this interaction, which involves the nitrogen of the amino group, may partially prevent the nucleophilic attack of the amino group to the CO_2 molecule. Finally, it is worth mentioning that if we consider a partial pressure low enough, such as 7 mbar, only carbamates are observed on SBA_DH by FTIR (Fig. 6). At this pressure, the quantity of CO_2 adsorbed by SBA_DH is 0.2 mmol/g (Fig. 4D) and this is in accordance with the maximum amount identified by the Dual-Site Langmuir model (n'_{max}).

The functionalization of the adsorbent has been obtained by impregnation, and DH molecules interact with the silica surface by means of intermolecular interactions, such as H-bonding and Van der Waals interactions. Nevertheless, the material is compatible with a regeneration through thermal treatment. When heated at a temperature suitable for the thermal regeneration of sorbents [18], such as 120 °C for 1 h, SBA_DH is stable, displaying a negligible mass loss (Fig. 7).

When comparing these results with those reported in the literature for similar sorbents (Table 3), it is worth noting that silica and tuff samples of previous studies have higher DH contents (30 wt% and 50–70 wt%, [13,16]), but result in adsorption capacities comparable to those obtained in this work (0.98–1.24 mmol/g compared to 0.89 mmol/g of this work). For the present work, an arbitrary amount of DH was incorporated, to prove the feasibility of the $scCO_2$-impregnation process; nevertheless, higher amounts of DH could be used for future studies. In addition, DH-functionalized sorbents reported in the literature require high-temperature regeneration (90–100 °C [13,14]) and not all of them (in particular MWCNTs) are thermally stable above 100 °C [14]. In conclusion, the material proposed here appears to be a promising starting point for the development of new CO_2 sorbents.

5. Conclusions

The results of this study show that supercritical CO_2 can be used as an alternative green solvent for the functionalization of silica with amino groups. This technique was successfully employed for the first time to the functionalization of silica with diaminohexane. The final sorbent has a SSA of 330 m^2/g, an average pore diameter of 6.1 nm and a pore volume of 0.7 cm^3/g. The content of diaminohexane is about 10 wt%. The functionalization appears to be homogeneous, and the sorbent is able to capture CO_2 through chemisorption and physisorption, both phenomena being reversible with a simple and rapid outgas at room temperature. The volumetric isotherm of CO_2 at RT is well described by a Dual-Site Langmuir model. Interestingly, the functionalized material is particularly effective in capturing CO_2 at low pressure, opening the way for possible applications in fields such as flue gas treatment and biogas enhancement [38]. Moreover, the sorbent appears to be compatible with thermal regeneration.

Finally, as future perspective, higher amounts of diaminohexane could be used for functionalizing silica, to explore and better exploit all the capabilities of this new class of CO_2 sorbents.

CRediT authorship contribution statement

Silvia Ronchetti: Writing – review & editing, Validation, Supervision, Resources, Funding acquisition. **Barbara Onida:** Writing – review & editing, Validation, Supervision, Resources, Methodology, Funding acquisition, Conceptualization. **Marta Gallo:** Writing – original draft, Methodology, Investigation, Data curation, Conceptualization. **Luigi Manna:** Writing – review & editing, Resources, Funding acquisition.

Declaration of Competing Interest

The authors declare that they have no known competing financial interests or personal relationships that could have appeared to influence the work reported in this paper.

Acknowledgements

The authors would like to acknowledge Eng. Francesca Chiofalo for her contribution in the experimental work and Prof. Marco Armandi for the support given for the volumetric and *in situ FTIR tests.*

APPENDIX A

Wide-angle XRD patterns (Figure A.1) of both SBA_ref and SBA_DH are characterized by three reflections typical of the 2D hexagonal mesoporous silica SBA-15 [39], i.e. (100) at 2θ equal to 0.88°, (110) at 2θ equal to 1.55° and (200) at 2θ equal to 1.78°. XRD spectra at high angles (Figure A.1B) do not reveal the presence of any crystalline phase, as expected [40].

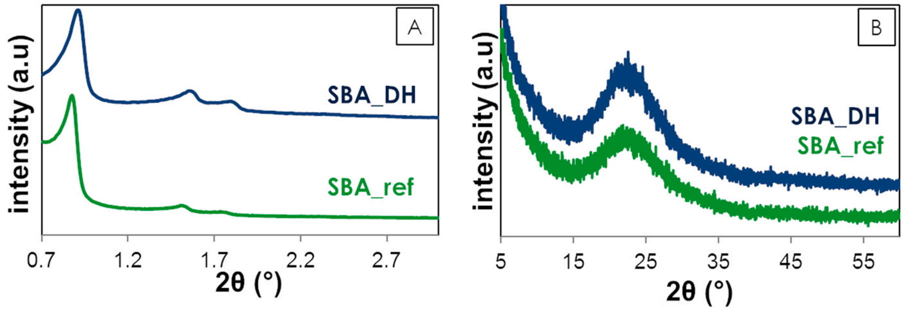

Figure A.1. XRD patterns at low (A) and high (B) angles of the reference sample, SBA_ref, and the functionalized sample, SBA_DH

The main properties of the sample impregnated by incipient wetness impregnation (SBA_DH_IWI) were obtained by nitrogen adsorption and TGA. These data are reported in Table A.1 with those of SBA_DH, as a comparison.

Table A.1
Textural properties and measured DH-content of the sample obtained by IWI, SBA_DH_IWI, and the $scCO_2$ functionalized sample, SBA_DH

	SBA_DH_IWI	SBA_DH
Specific surface area (m^2/g)	270	330
Pore volume (cm^3/g)	0.5	0.7
Measured DH-content (%)	8.2	11.2

Data availability

Data will be made available on request.

References

[1] NOAA (National Oceanic and Atmospheric Administration), Carbon dioxide now more than 50% higher than pre-industrial levels. ⟨www.noaa.gov⟩. 2022.
[2] Intergovernmental Panel on Climate Change (IPCC), "Sixth Assessment Report (2023)", ⟨https://www.ipcc.ch/ar6-syr/⟩ (accessed 19/09/2024).
[3] J. Hack, N. Maeda, D.M. Meier, Review on CO_2 capture using amine-functionalized materials, ACS Omega 7 (44) (2022) 39520–39530, https://doi.org/10.1021/acsomega.2c03385.
[4] D.-M. D'Alessandro, B. Smit, J.-R. Long, Carbon dioxide capture: prospects for new materials, Angew. Chem. Int. Ed. 49 (2010) 6058, https://doi.org/10.1002/anie.201000431.
[5] V. Gupta, P. Mobley, J. Tanthana, L. Cody, D. Barbee, J. Lee, R. Pope, M. Lail, J. Thornburg, R. Chartier, Aerosol emissions from water-lean solvents for post-combustion CO_2 capture, Int. J. Greenh. Gas. Control 106 (2021) 103284, https://doi.org/10.1016/j.ijggc.2021.103284.
[6] F. Meng, Y. Meng, T. Ju, S. Han, L. Lin, J. Jiang, Research progress of aqueous amine solution for CO_2 capture: a review, Renew. Sustain. Energy Rev. 168 (2022) 112902, https://doi.org/10.1016/j.rser.2022.112902.
[7] A. Samanta, A. Zhao, G.-K.-H. Shimizu, P. Sarkar, R. Gupta, Post-combustion CO_2 capture using solid sorbents: a review, Ind. Eng. Chem. Res. 51 (2012) 1438, https://doi.org/10.1021/ie200686q.
[8] S. Kundu, T. Khandaker, M.A.A.M. Anik, M.K. Hasan, P.K. Dhar, S.K. Dutta, M. A. Latif, M.S. Hossain, A comprehensive review of enhanced CO_2 capture using activated carbon derived from biomass feedstock, RSC Adv. 14 (2024) 29693, https://doi.org/10.1039/d4ra04537h.
[9] E. Pérez-Botella, S. Valencia, F. Rey, Zeolites in adsorption processes: state of the art and future prospects, Chem. Rev. 122 (24) (2022), https://doi.org/10.1021/acs.chemrev.2c00140.
[10] L. Santamaría, S.A. Korili, A. Gil, Layered double hydroxides for CO2 adsorption at moderate temperatures: synthesis and amelioration strategies, Chem. Eng. J. 445 (2023) 140551, https://doi.org/10.1016/j.cej.2022.140551.
[11] A. Danon, P.C. Stair, E. Weitz, FTIR study of CO_2 adsorption on amine-grafted SBA-15: elucidation of adsorbed species, J. Phys. Chem. C. 115 (23) (2011) 11540–11549.
[12] P. Singh, J.P.M. Niederer, G.F. Versteeg, Structure and activity relationships for amine based CO_2 absorbents, Int J. Greenh. Gas. Control 1 (1) (2007) 5–10, https://doi.org/10.1016/S1750-5836(07)00015-1.
[13] G.-G. Kaya, Diamine functionalized volcanic tuff: a promising CO_2 adsorbent, J. Chem. Technol. Biotechnol. 98 (10) (2023) 2489, https://doi.org/10.1002/jctb.7474.
[14] N.-S. Ardali, S. Riahi, M. Abbasi, N. Mohammadpour, Experimental investigation of carbon dioxide adsorption using functionalized MWCNTs with 1,6-diaminohexane, Fuel 338 (2023) 127213, https://doi.org/10.1016/j.fuel.2022.127213.
[15] P. Singh, D.W.F. Brilman, M.-J. Groeneveld, Solubility of CO_2 in aqueous solution of newly developed absorbents, Energy Procedia 1 (1) (2009) 1257, https://doi.org/10.1016/j.egypro.2009.01.165.
[16] E.-S. Sanz-Pérez, A. Arencibia, R. Sanz, G. Calleja, New developments on carbon dioxide capture using amine-impregnated silicas, Adsorption 22 (2016) 609, https://doi.org/10.1007/s10450-015-9740-2.
[17] R. Girimonte, F. Testa, M. Turano, G. Leone, M. Gallo, G. Golemme, Amine-Functionalized mesoporous silica adsorbent for CO_2 capture in confined-fluidized bed: study of the breakthrough adsorption curves as a function of several operating variables, Processes 10 (2022) 422, https://doi.org/10.3390/pr10020422.
[18] R. Girimonte, F. Testa, M. Gallo, R. Buscieti, G. Leone, B. Formisani, Adsorption of CO2 on amine-modified silica particles in a confined-fluidized bed, Processes 8 (2020) 1531, https://doi.org/10.3390/pr8121531.
[19] S. Brunauer, P.H. Emmett, E. Teller, Adsorption of gases in multimolecular layers, J. Am. Chem. Soc. 60 (1938) 309–319, https://doi.org/10.1021/ja01269a023.
[20] E.P. Barrett, L.G. Joyner, P.P. Halenda, The determination of pore volume and area distributions in porous Substances". I. Computations from nitrogen isotherms, J. Am. Chem. Soc. 73 (1951) 373–380, https://doi.org/10.1021/ja01145a126.
[21] G. SocratesInfrared and Raman characteristic group frequencies: tables and charts. 2001.
[22] B. Onida, S. Fiorilli, L. Borello, G. Viscardi, D. Macquarrie, E. Garrone, Mechanism of the optical response of mesoporous silica impregnated with reichardt's dye to NH3 and other gases, J. Phys. Chem. B 108 (2004) 16617–16620, https://doi.org/10.1021/jp037094u, 2-s2.0-8344259898.
[23] Bergna H.E. The Colloid Chemistry of Silica. Comstock, J., Ed., Advances in Chemistry Series. 1994. 234. American Chemical Society, Washington DC. doi:10.1021/ba-1994-0234.
[24] M. Thommes, K. Kaneko, A.V. Neimark, J.P. Olivier, F. Rodriguez-Reinoso, J. Rouquerol, K.S.W. Sing, Physisorption of gases, with special reference to the evaluation of surface area and pore size distribution (IUPAC Technical Report), Pure Appl. Chem. 87 (2015) 1051–1069, https://doi.org/10.1515/pac-2014-1117.
[25] M. Castiglioni, L. Rivoira, M. Gallo, I. Ingrando, M. Del Bubba, B. Onida, M. C. Bruzzoniti, Removal of sugars from food and beverage wastewaters by amino-modified SBA-15, J. Clean. Prod. 324 (2021) 129236, https://doi.org/10.1016/j.jclepro.2021.129236.
[26] H. Swenson, N.P. Stadie, Langmuir's theory of adsorption: a centennial review, Langmuir 35 (2019) 5409–5426, https://doi.org/10.1021/acs.langmuir.9b00154.
[27] R. Sips, On the structure of a catalyst surface, J. Chem. Phys. 16 (5) (1948) 490–495, https://doi.org/10.1063/1.1746922.
[28] O. Redlich, D.L. Peterson, A useful adsorption isotherm, J. Phys. Chem. 63 (6) (1959) 1024–10214, https://doi.org/10.1021/j150576a611.
[29] C.J. Radke, J.M. Prausnitz, Thermodynamics of multi-solute adsorption from dilute liquid solutions, AIChE J. 18 (4) (1972) 761–768, https://doi.org/10.1002/aic.690180418.
[30] J. Tóth, State equations of the solid–gas interface layers, Acta Chim. Acad. Sci. Hung. 69 (3) (1971) 311–317.
[31] A.W. Marczewski, M. Jaroniec, A new isotherm equation for heterogeneous solid surfaces, Pol. J. Chem. 57 (1983) 1093–1103.

[32] W. Fritz, E.U. Schlunder, Simultaneous adsorption equilibria of organic solutes in dilute aqueous solutions on activated carbon, Chem. Eng. Sci. 29 (5) (1974) 1279–1282, https://doi.org/10.1016/0009-2509(74)85020-8.

[33] C. Zanzottera, M. Armandi, S. Esposito, E. Garrone, B. Bonelli, CO_2 adsorption on aluminosilicate Single-Walled nanotubes of imogolite type, J. Phys. Chem. C. 116 (38) (2012) 20417–20425, https://doi.org/10.1021/jp3061637.

[34] M. PavaniOrganosilici a mesoporosità controllata per la cattura e la conversione dell'anidride carbonica". MS Thesis. Politecnico di Torino. 2013.

[35] C. Knofel, C. Martin, V. Hornebecq, P. Llewellyn, Study of carbon dioxide adsorption on mesoporous aminopropylsilane-functionalized silica and titania combining microcalorimetry and in situ infrared spectroscopy, J. Phys. Chem. C. 113 (2009) 21726–21734, https://doi.org/10.1021/jp907054h.

[36] A.C. Forse, P.J. Milner, New chemistry for enhanced carbon capture: beyond ammonium carbamates, Chem. Sci. 12 (2021) 508–516, https://doi.org/10.1039/D0SC06059C.

[37] S. Sircar, Pressure swing adsorption, Ind. Eng. Chem. Res. 41 (6) (2002) 1389–1392, https://doi.org/10.1021/ie0109758.

[38] H.N.A. Halim, V. Rajiman, A.M. Shariff, A review on CO_2 absorption using chemical solvents at low and high CO_2 partial pressure conditions in a packed column, Open Chem. Eng. J. 16 (2022), https://doi.org/10.2174/18741231-v16-e2204140.

[39] V. Meynen, P. Cool, E.F. Vansant, Verified syntheses of mesoporous materials, Microporous Mesoporous. Mater. 125 (2009) 170–223, https://doi.org/10.1016/j.micromeso.2009.03.046.

[40] M. Gallo, L. Serpella, F. Leone, L. Manna, M. Banchero, S. Ronchetti, B. Onida, Piroxicam loading onto mesoporous silicas by supercritical CO_2 impregnation, Molecules 26 (2021) 2500, https://doi.org/10.3390/molecules26092500.